

## Observation of crustal deformation by means of wellhead pressure monitoring

H. Woith<sup>\*</sup>, A.P. Venedikov<sup>\*\*</sup>, C. Milkereit<sup>\*</sup>, M. Parlaktuna<sup>\*\*\*</sup>, A. Pekdeger<sup>\*\*\*\*</sup>

<sup>\*</sup>GeoForschungsZentrum Potsdam, <sup>\*\*</sup>Geophysical Institute & Central Laboratory on Geodesy, Sofia, <sup>\*\*\*</sup>Middle East Technical University, Ankara, <sup>\*\*\*\*</sup>FU Berlin, Berlin.

### Abstract.

The paper represents results from a wellhead station, installed in a 400 m deep artesian well, drilled in the city of Bursa, NW part of Turkey. Water pressure variations are measured by a borehole sensor at a mean pressure level of 1.6 bars. The air-pressure variations are measured in parallel at the surface next to the borehole. The data processed is a series of 421 days (29.04.2004 – 23.06.2005) 5-minutes ordinates. The station is situated in a strongly dangerous seismic region, surrounded by a set of seismic stations. The main objective of the observations is the study of non-tidal signals in pore-pressure related to earthquakes, possibly event precursors. The paper shows how to process the data, in order to reveal anomalies in the residuals, which can be studied as such signals. Namely, the original data are reduced by: (i) a well determined tidal signal, (ii) the effect of the external air-pressure, by using an appropriate model, (iii) a simple polynomial model of the drift and (iv) some annual meteorological waves with basic frequency 1 cycle/year. The estimation and the reduction are made by the tidal program VAV, solving a system of equations by the least squares method, dealing at once in parallel with all components.

### 1. Introduction.

The paper represents preliminary analysis results from the water pressure records in a wellhead station. The station is installed in a 400 m deep artesian well, drilled in the city of Bursa, NW part of Turkey (Figure 1).

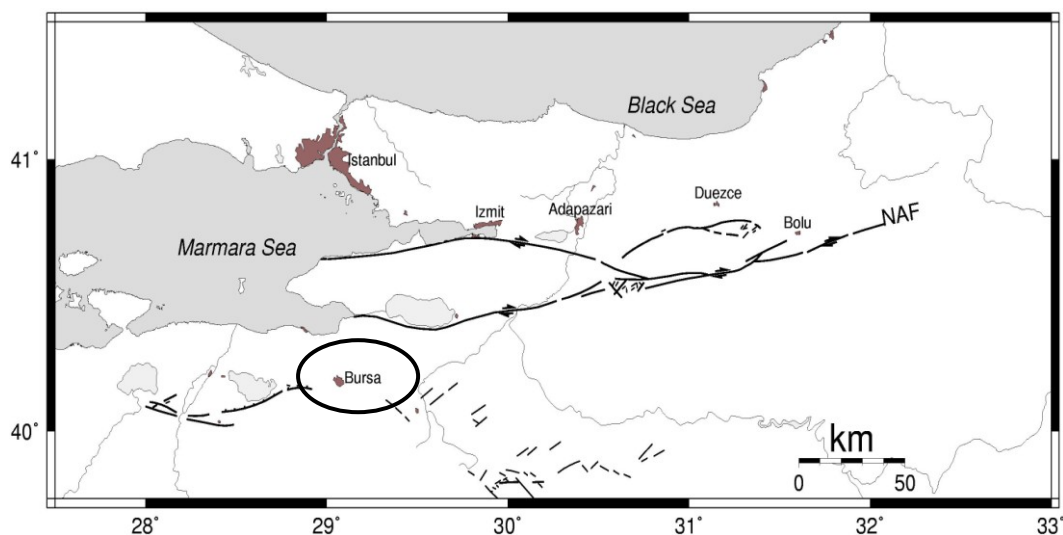


Figure 1. Location of the station in the city of Bursa for wellhead pressure monitoring.

Absolute pressure variations are measured by a borehole pressure sensor at a mean pressure level of 2.6 bars. A second sensor provides relative water pressure, at a mean level of 1.6 bar, the effect of the air-pressure being mechanically reduced (Figure 2).

Air-pressure variations are measured in parallel at the surface a few meters away from the borehole, in order to study their direct and indirect effect on the data.

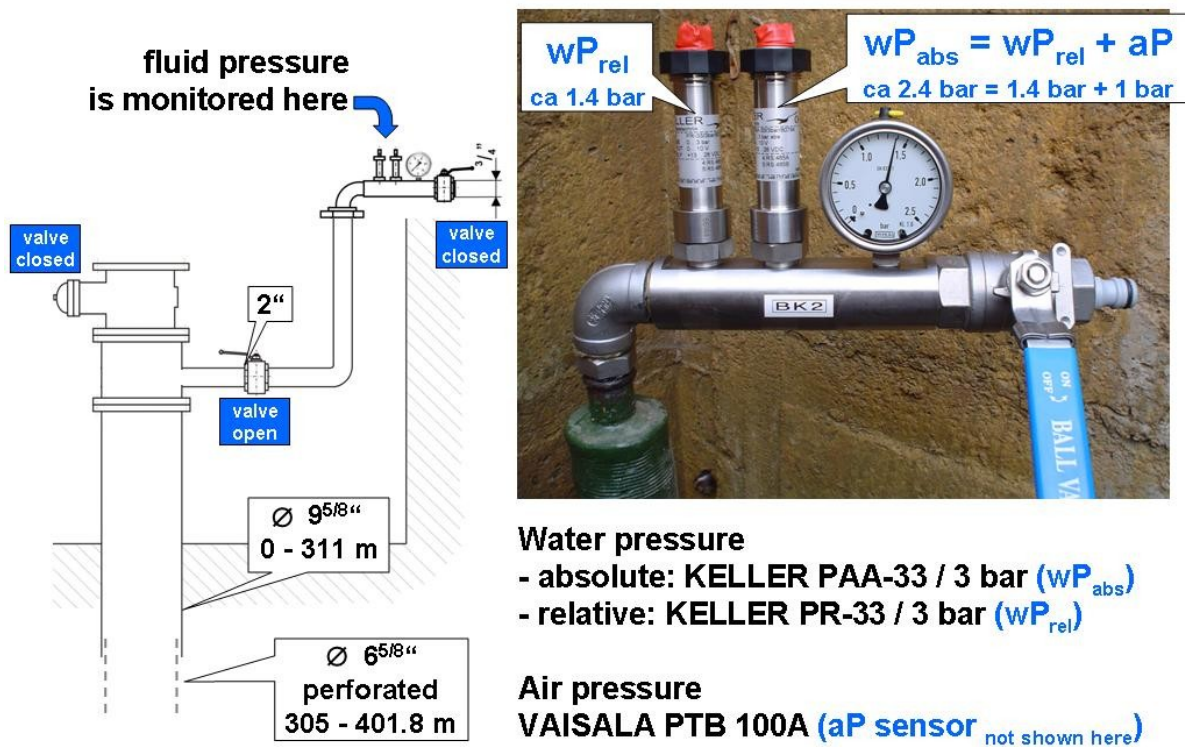


Figure 2 Technical setup of the wellhead pressure monitoring.

The data processed is a series of 421 days (29.04.2004 – 23.06.2005) 5-minutes ordinates. Figure 3 gives an idea about the quality and the properties of the data.

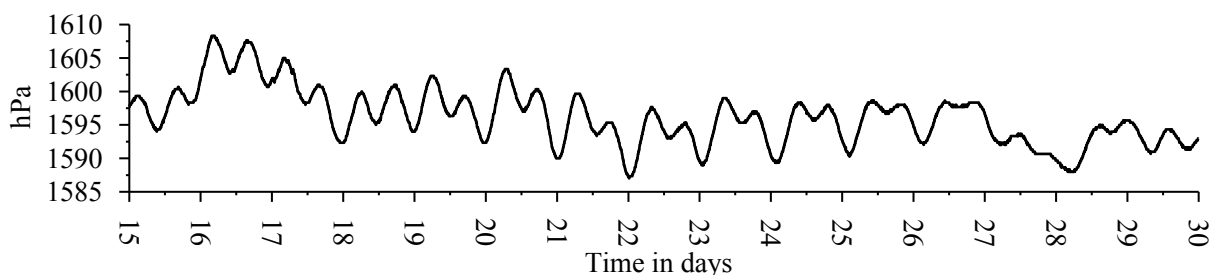


Figure 3. Sample of 15 days of the recorded 5-minutes data.

The station is situated in an active seismic region. The main objective of the investigation is the study of non-tidal signals in pore-pressure related to earthquakes and its potential as earthquake precursors.. This task needs at first place high quality tidal data with an as good as possible determination of the tidal signal and thus - as good as possible separation of the non-tidal signals.

The aims of the investigation need also the reduction of the meteorological effects. The effect of the air-pressure is taken into account by a multi-channel and a cross-regression analysis, by using an appropriate model.

The temperature variations now are not included in the data and. Instead, their effect is reduced by including in the processing annual components with basic frequency 1 cycle/year.

**3. General model applied by the VAV program.**

The algorithm of VAV (Venedikov et al., 2004) is based on the partition of the data in a set of intervals without overlapping  $I(T)$  with central epoch  $T = T_1, T_2, \dots T_N$  and length  $\Delta = \dots - \dots$  hours (when there are no gaps). Independently in every  $I(T)$  the drift of the data is represented by a polynomial of power  $K_d$ .

In this case a most simple but rather efficient variant is used with  $\Delta T = 24^h$  and  $K_d = \dots$ . This variant is accompanied by a determination of the LP tides in parallel with the other tidal groups. For the LP tides a single group Mf is used (Ducarme et al., 2004).

Since the data are taken every 5 min., every  $I(T)$  covers 288 consecutive 5-minutes data.

The data in the  $I(T)$  are transformed into a set of complex filtered quantities, by using

$$u_v(t) = \sum_{\tau} \dots = \dots = \dots \dots \dots \quad (1)$$

where  $\tau$  is internal time in the  $I(T)$ , which vary from  $-717.5^m$  to  $+717.5^m$  through  $5^m$ .

When dealing with the quantities  $u(T)$  obtained by (1) for every dsy, the time  $T$  is expressed in days

The filtration is made by using a set of orthogonal filters  $F_v(\tau)$ , which are complex functions of the internal time  $\tau$ . For the case here used  $\Delta = \dots$  s = 1 day and  $K_d = \dots$  the filters are the Fourier operators

$$F_v(\tau) = \left( \dots \right) = \dots \dots \dots \quad (2)$$

The filters  $F_v(\tau)$  eliminate an arbitrary constant, i.e. a polynomial of power  $K_d = 0$ .

In connection with the concrete task, VAV uses the so called zero option (Venedikov et al., 2004), used also for the study of the polar motion (Ducarme et al., 2005, 2006), which includes in the set (1) a zero filtered number  $u_0(T)$ . The latter is a real number, equal to the arithmetic mean of the data in  $I(T)$ .

Further VAV creates a system of observational equations about the filtered numbers, which generally looks like

$$\left. \begin{aligned} u_1(T) &= \dots + \dots \\ u_2(T) &= \dots + \dots \\ \dots & \dots \dots \dots \\ u_6(T) &= \dots + \dots \\ u_0(T) &= \dots + \dots + \dots + \dots \end{aligned} \right\} \dots \dots \dots \quad (3)$$

Here  $S_{\nu}^{(T)}$   $\nu =$  is the model of the tidal signal, used in the tidal analysis. As said above, this model includes a common LP tidal group MF (Ducarme et al., 2004). The terms  $M_{\nu}^{(T)}$   $\nu =$   $>$  represents the multi-channel model used by VAV for the frequency dependent effect of the air-pressure on the D, SD, ... filtered numbers  $u_{\nu}^{(T)}$  for  $\nu >$  .

The term  $M_0(T)$ , together with the terms  $D(T)$  &  $A(T)$  are included in the model of  $u_0(T)$  because the corresponding filter (arithmetic mean), unlike the filters  $F_{\nu}^{(T)}$  for  $\nu >$  , does not eliminate the drift and the slow meteorological effects. Concretely,  $M_0(T)$  is a particular model of the effect of the effect of the air-pressure,  $D(T)$  is a polynomial model of the drift, i.e. its manifestation in the central epochs  $T$  and  $A(T)$  is a term, represented low frequency meteorological effect, mainly connected with the annual variations of the temperature.

After the joint solution of the system (3) we get the adjusted quantities  $\tilde{u}_{\nu}^{(T)}$   $\tilde{u}_{\nu}^{(T)}$   $\tilde{D}(T)$  &  $\tilde{A}(T)$  respectively. They are used to get for every day the residuals of the zero filtered number

$$\Delta_{\nu} = \tilde{u}_{\nu}^{(T)} - \tilde{u}_{\nu}^{(T)} \quad (4)$$

where we expect to find particular anomalies as signals, which can be studied as potential earthquake precursors.

#### 4. The tidal signal $S_{\nu}^{(T)}$ .

With respect to the tidal signal  $S_{\nu}^{(T)}$ , the common solution of (3), including the equations for  $u_0(T)$ , does not create particular problems. As said above, it is necessary to include an LP group MF, as it is done by (Ducarme et al., 2004).

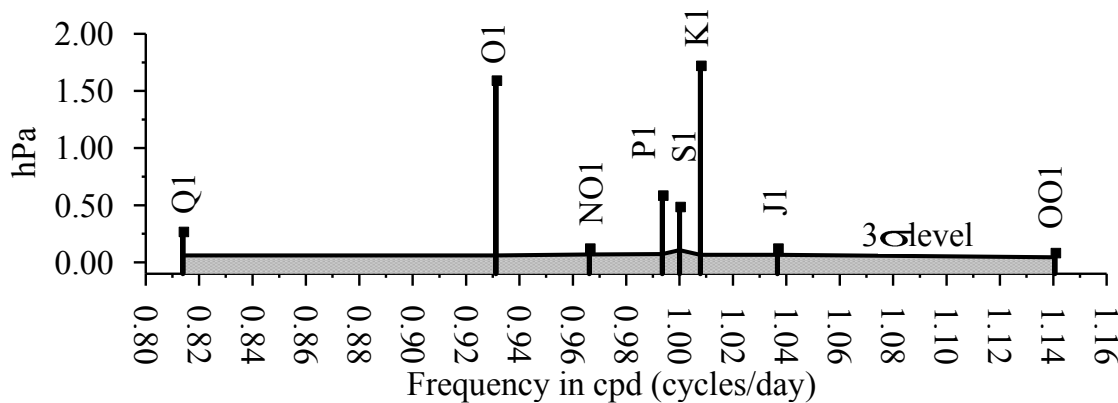


Figure 4. Estimated amplitudes of the main D tides with the  $3\sigma$  confidence level, where  $\sigma$  denotes RMS (root mean square error) of the corresponding amplitudes.

Figures 4 & 5 show the estimated D and SD amplitudes of the main tides. The comparison with the  $3\sigma$  level, which is a rather high level, shows that all amplitudes are certainly statistically significant. Thus we dispose by rather satisfactory results, which testify for a good quality of the data.

The result, obtained for the amplitude of the MF tide is  $0.406 \pm 0.124$  hPa, i.e. even for the LP tides we get statistically significant result with confidence probability higher than 95%.

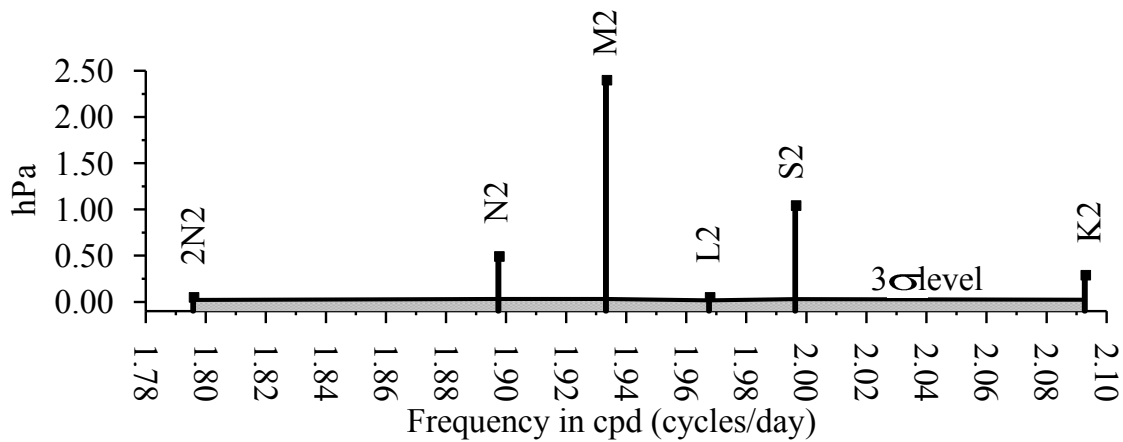


Figure 5. Estimated amplitudes of the main SD tides with the  $3\sigma$  confidence level.

Figure 6 shows the data  $u_0(T)$  reduced by the estimated effect of the tidal signal  $S(T)$ , i.e. the non-tidal component of the data, usually considered as the drift of the data.

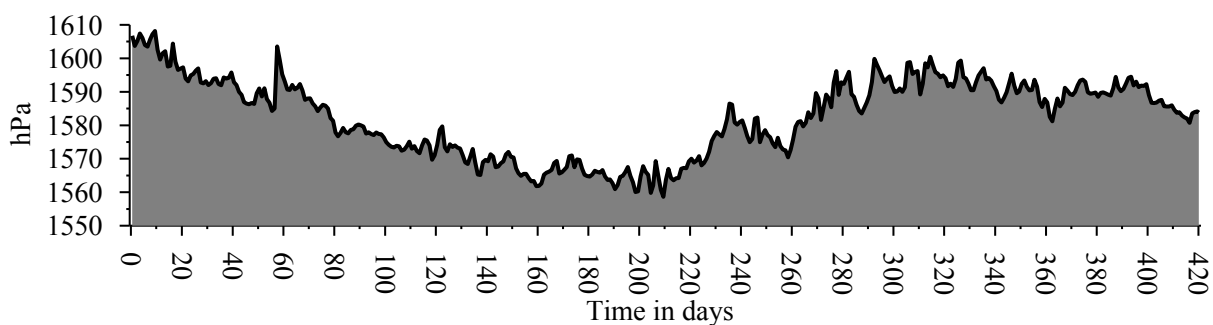


Figure 6. The non-tidal component of the data as partial residual  $u_0(T) - \tilde{u}_0(T)$ .

#### 4. The effect of the air-pressure $M_0(T)$ .

The model used for  $M_0(T)$  is the following. We set up

$$M_0(T) = R_p p(T - \Delta) - \Delta \tag{5}$$

where  $p(T - \Delta)$  is the air-pressure at time  $T - \Delta$ ,  $\Delta$  is unknown time lag, positive for retardation and  $R_p$  is unknown regression coefficient.

The problem of using this model in (3) is that the unknown  $\Delta$  enters non-linearly in the equations, i.e. it cannot be estimated by the LS. This problem has been solved by solving the system (3) for a set of values of  $\Delta$  and thus obtaining  $R_p = R_p(\Delta)$  as a function of  $\Delta$ , looking for the minimum of this function. As shown by Figure 6, the minimum has been found at  $\Delta = -2$ , i.e. for 2 hours of advance. Once fixed the value  $\Delta = -2$ , there were no more problems for solving (3) by the LS.

The estimate of the regression coefficient obtained is

$$R_p = - \pm \text{(hPa in water)/ hPa air-pressure at the surface} \tag{6}$$

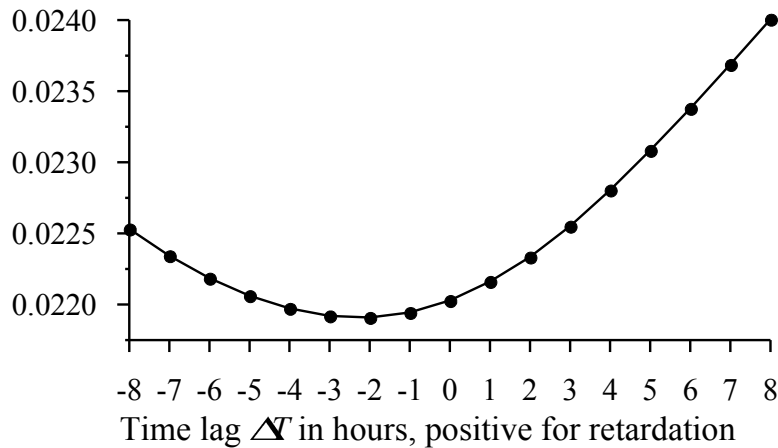


Figure 7. RMS of the regression coefficient  $R_p = \dots \Delta$  as a function of  $\Delta$ .

In the next Figure 8, the data  $u_0(T)$  are reduced by the tidal signal, as well as by the effect of the air-pressure  $M_0(T)$ .

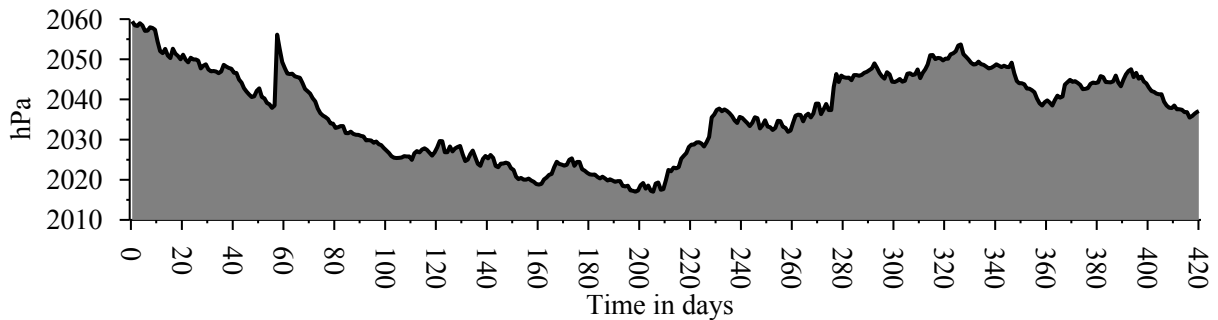


Figure 8. Partial residuals  $u_0(T) - \dots$ .

The comparison between Figure 6 and Figure 8 show that the inclusion of  $M_0(T)$  is efficient, because we get a better smoothed curve, in which a lot of small anomalies, which could be misleading, are suppressed.

### 5. Polynomial component and annual component.

For the polynomial component  $D(T)$  we have chosen the simple model

$$D(T) = \dots + \dots + \dots \tag{7}$$

with unknown coefficients  $b_j$ . Using higher powers of (7) appeared to be not suitable, first, in order to observe the principle of the parsimony and second, because they interfere with the annual component. Namely, when high powers are used, we start getting unreasonably great amplitudes of the annual component.

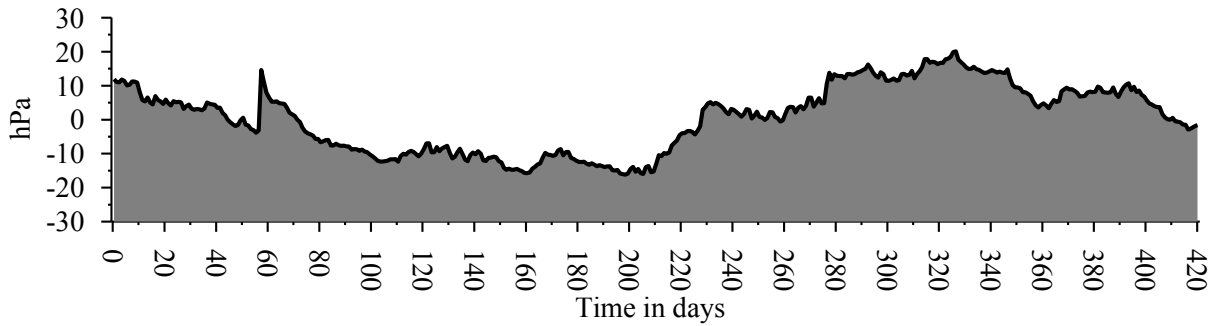


Figure 9. Partial residuals  $u_0(T) - \tilde{u}_0(T)$

Figure 9 shows the effect of  $D(T)$ , which is mainly a reduction of the curve to the horizontal zero line.

For the annual component  $A(T)$ , by having in mind the length of the data (421 days), as well as that  $A(T)$  is designed to represent some meteorological phenomena, mainly the temperature variations, we have used a Fourier series with basic period one year. An optimum has been obtained to go till order 4, i.e. we have applied

$$A(T) = \sum_{k=1}^4 \left[ \alpha_k \cos\left(\frac{2\pi k T}{365}\right) + \beta_k \sin\left(\frac{2\pi k T}{365}\right) \right] \quad (8)$$

with unknowns  $\alpha_k$  &  $\beta_k$  and the time  $T$  expressed in days.

Figure 10 shows the final result of the reduction of the data, after  $A(T)$  had joint the other reduced components. The comparison with Figures 6, 7 and 8 shows that  $A(T)$  has a rather important effect.

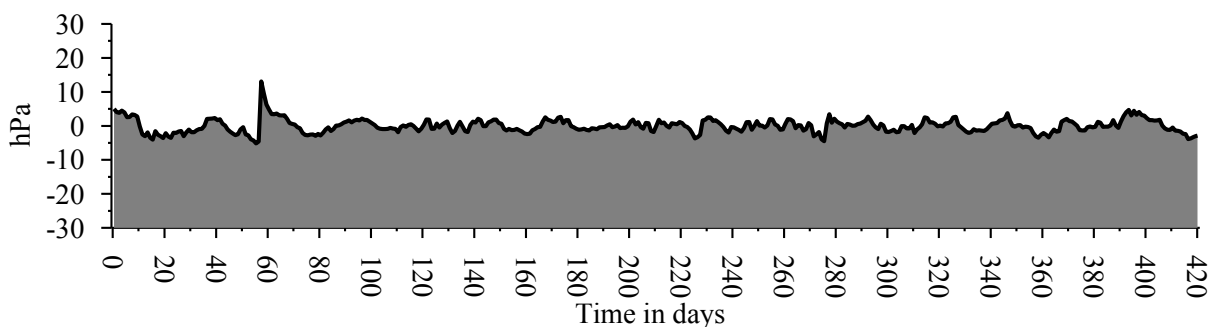


Figure 10. Finally obtained residuals  $\Delta u = u_0(T) - \tilde{u}_0(T) - \tilde{u}_1(T) - \tilde{u}_2(T) - \tilde{u}_3(T) - \tilde{u}_4(T)$  after the LS solution of the system (3).

### 6. Final representation and conclusions.

Figure 11 uses an elementary way to better visualize the residuals, namely by plotting their absolute values. This is possible because when we are studying the anomalies, it makes no difference whether they are positive or negative.

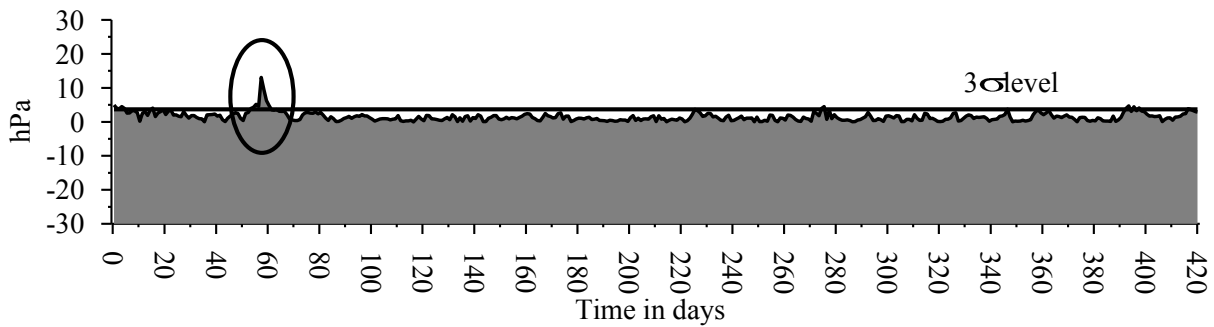


Figure 11. Absolute residuals  $|\Delta$  and a  $3\sigma$  threshold level.

More essential is that in such cases we have to use statistical criteria. In Figure 11 the criterion used is the  $3\sigma$  level, where  $\sigma$  is computed as

$$\sigma = \sqrt{\frac{\sum r^2}{n_{\Delta}}} \quad (9)$$

where  $n_{\Delta}$  is the number of the residuals.

When given  $|\Delta|$  exceeds this level we can firmly believe that it is an anomalous residual with a high enough confidence probability.

Thus Figure 11 allowed us to clearly distinguish an anomaly, surrounded by a circle.

The aims of the paper are to show one way for a careful analysis of the data, when their purpose is the difficult problem for finding earthquake precursors. At the first place we need high quality of data from which we can obtain reliable tidal signal, in order to eliminate it. Further we have to carefully create regression models for other components, like here for the air-pressure, polynomial component and annual terms.

We would like to emphasize that the use of one and the same program for the solution of the purely tidal and non-tidal tasks is corresponding to a fundamental LS principle. According to the LS principle it is necessary to include simultaneously in one common system of equations, like (3), all models and get in parallel the estimate of all unknowns.

In practice very often this LS principle is violated by estimating and subtracting consecutively and independently the components, whose effect has to be reduced.

The series of data here used is experimental and very short for checking whether the anomaly in Figure 11 is really related to an earthquake or not. Such conclusion needs much larger experimental material and sophisticated statistics, studying the relation between a great number of anomalies and seismic events.

**References.**

1. Ducarme B., Venedikov A.P., Arnos J., Vieira R., 2004. Determination of the long period tidal waves in the GGP superconducting gravity data. *Journal of Geodynamics*, **38**, 307-324.
2. Ducarme B., Van Ruymbeke M., Venedikov A.P., Arnos J., Vieira R., 2005. Polar motion and non-tidal signals in the superconducting gravimeter observations in Brussels. *Bulletin d'Informations des Marées Terrestres*, **140**, 11153-11171.
3. Ducarme B., Venedikov A.P., Arnos J., Chen X.D., Sun H.P., Vieira R., 2006. Global analysis of the GGP superconducting gravimeters network for the estimation of the polar motion effect on the gravity variations. *Journal of Geodynamics*, **41**, 334-344.
4. Venedikov A.P., Vieira R., 2004. Guidebook for the practical use of the computer program VAV – version 2003. *Bulletin d'Informations des Marées Terrestres*, **139**, 11037-11102.